

# THREE-PHASE INCLUSIONS IN EMERALD AND THEIR IMPACT ON ORIGIN DETERMINATION

Sudarat Saeseaw, Vincent Pardieu, and Supharat Sangsawong

Until now, the observation of three-phase inclusions in emeralds has been considered a potential indicator of Colombian origin. Nevertheless, emeralds from Afghanistan (Panjshir Valley), China (Davdar), and Zambia (Kafubu and a new deposit at Musakashi) may contain three-phase inclusions resembling those often found in specimens from Colombian deposits (Muzo, Chivor, La Pita, Coscuez, and Peñas Blancas). This article presents detailed photomicrographs of samples from these localities, with a focus on their multiphase inclusions. Also investigated are spectroscopic features and trace-element data. For the gemologist studying the origin of emeralds hosting three-phase inclusions, a powerful set of tools to aid in this determination comes from the combination of detailed microscopic examination, UV-Vis-NIR and FTIR spectroscopy, and LA-ICP-MS trace-element analysis.

The traditional practice of assigning Colombian origin to emeralds exhibiting three-phase inclusions (Giuliani et al., 1993) is in need of updating, as we now know that such inclusions are often seen in emeralds from other locations, including China, Zambia (Schwarz and Pardieu, 2009), and Afghanistan (Hammarstrom, 1989; Bowersox et al., 1991). The characterization of these inclusions using spectroscopy and chemical composition has not been documented until now.

A new Zambian deposit at Musakashi was first reported in 2005 (Zwaan et al., 2005), and field trip reports were subsequently published (Klemm, 2009 and 2010). These articles presented historical and geological information about the mine (see box A), examined the gemological properties of these new emeralds, and presented chemical analysis using electron microprobe (Zwaan et al., 2005).

The present study characterizes emeralds containing multiphase inclusions from all of the localities above by using microscopy, spectroscopy, and trace-element analysis to create a framework for geographic origin determination.

See end of article for About the Authors and Acknowledgments.

GEMS & GEMOLOGY, Vol. 50, No. 2, pp. 114–132,  
<http://dx.doi.org/10.5741/GEMS.50.2.114>.

© 2014 Gemological Institute of America

## MATERIALS AND METHODS

A total of 84 emeralds were studied, gathered from the GIA Field Gemology Collection and from gem merchants of Zambian and Colombian emeralds. Color ranged from light to deep green. The samples were studied in three forms: 55 were rough samples with one or two polished surface windows, 28 were fabricated as optical wafers oriented either perpendicular or parallel to the crystal's c-axis, and one was faceted. After fabrication, the samples ranged from 0.18 to 4.85 ct. The group consisted of:

- Eleven samples reportedly from Musakashi (figure 1), acquired from gem dealer Guy Clutterbuck, who visited the mines several times. Weight range: 0.57–4.85 ct.
- Ten samples collected from the Kagem mine in the Kafubu area of Zambia by author VP in the summer of 2013. Weight range: 0.29–2.22 ct.
- Fifteen samples collected from Afghanistan's Panjshir Valley by author VP in 2011. Weight range: 0.18–1.80 ct.
- Thirteen samples collected from Davdar, China, by author VP in 2005 and 2009. Weight range: 0.16–1.77 ct.
- Thirty-five Colombian samples from Muzo (12), Coscuez (12), La Pita (3), Peñas Blancas (2), and Chivor (6), acquired from Flavie Isatelle, a



Figure 1. These emeralds from Musakashi, Zambia, range from 0.57 to 4.85 ct. The rough samples were polished with one window on each. The faceted sample measures  $6.29 \times 5.35 \times 3.53$  mm and weighs 0.97 ct. Photo by N. Kitdee.

field gemologist/geologist who visited in May 2010, and gem merchant Ron Ringsrud. Weight range: 0.12–4.14 ct.

Standard gemological properties were measured with a Rayner refractometer (yttrium-aluminum-garnet prism) equipped with a near sodium-equivalent light source to measure refractive index and birefringence, a Chelsea filter, and four-watt long-wave (365 nm) and short-wave (254 nm) UV lamps to observe fluorescence. Due to fracturing in the samples, coupled with their relatively small sizes, no useful specific gravity measurement was acquired. The wafers' optical path lengths were measured using a Mitutoyo Series 395 spherical micrometer with an accuracy of 2 microns. Microscopic examination was performed with GIA binocular microscopes at  $10\times$ – $70\times$  magnification, using both darkfield and brightfield illumination. Other lighting techniques, including fiber-optic illumination, were employed to investigate internal characteristics. Photomicrographs were captured at up to  $180\times$  magnification with a Nikon SMZ 1500 sys-

tem using darkfield, brightfield, and oblique illumination with a fiber-optic light.

Ultraviolet through visible and near-infrared (UV-Vis-NIR) spectra were collected with a Hitachi U-2900 spectrophotometer (for polarized ordinary ray spectra) at 1 nm resolution and a PerkinElmer Lambda 950 spectrophotometer at 0.3 nm resolution, operating with a 60 mm integrating sphere accessory and a Lambda polarizer accessory. Fourier-transform infrared (FTIR) spectroscopy was performed using a Thermo Nicolet 6700 FTIR spectrometer operating with a  $4\times$  beam condenser accessory at  $4\text{ cm}^{-1}$  resolution. A Renishaw inVia Raman microscope fitted with a 514 nm argon ion laser was used for identifying inclusions.

For laser ablation-inductively coupled plasma-mass spectrometry (LA-ICP-MS) chemical analysis, we used a Thermo Scientific X Series II ICP-MS combined with a Nd:YAG-based laser ablation device operating at a wavelength of 213 nm. For the ICP-MS operations, the forward power was set at 1300 W and the typical nebulizer gas flow was approximately

## BOX A: EMERALDS FROM MUSAKASHI, ZAMBIA

Little information is available about the Musakashi deposit (figure A-1) reportedly discovered in 2002, and much of it is conflicting. It appears to have originally been worked by local miners from 2002 to 2004. Emeralds from Musakashi were first reported in 2005 by Antonin Seifert, Stanislav Vrána, Björn Anckar, and Jaroslav Hyršl (Zwaan et al., 2005). Seifert and his colleagues reported that these emeralds had a significantly different color from those found in the Kafubu area. The Musakashi stones were said to show an intense bluish green reminiscent of emeralds from Muzo, Colombia. The similarity did not end there:

The most interesting characteristic was the presence in all the stones of three-phase inclusions, consisting of a bubble and a cube-shaped crystal in a liquid, almost identical to those commonly seen in Colombian emeralds.

Zwaan et al. also identified sphene, iron oxides, feldspar, and quartz as mineral inclusions.

Production reportedly resumed in 2006, starting with hand tools and progressing to the use of an excavator for a few months in 2009 (Klemm, 2009 and 2010). These reports, published after visits to Musakashi in July 2009 and August 2010, provide details adding to the history of emerald mining there.

### Location and Access

During the dry season, the Musakashi area is accessible by a five-hour, 165 km (102 mile) drive from Ndola, mainly on the poorly maintained Kasempa road (Klemm, 2009 and 2010).

### Production and Distribution

According to the mine director, the area produced about 15–20 kg of emeralds from its discovery through late 2010 (Klemm, 2010). Gem merchant Guy Clutterbuck, who supplied some of the samples for this study, reported to one of the authors in 2013 and 2014 that limited emerald mining was still taking place near Musakashi.



Figure A-1. This map shows the location of the Kafubu and the Musakashi emerald deposits.

0.90 L/min. The carrier gas used in the laser ablation unit was He, set at approximately 0.78 L/min. The alignment and tuning sequences were set to maximize Be counts and keep the ThO/Th ratio below 2%. Laser ablation conditions consisted of a 40  $\mu\text{m}$  diameter laser spot size, a fluence of  $10 \pm 1 \text{ J/cm}^2$ , and a 7 Hz repetition rate. For quantitative analysis, samples must be calibrated against an external standard of known composition, which meant measuring the signals for the elements of interest in the sample and comparing them to the signals for a standard with known concentrations of those elements. Generally, NIST 610 and 612 glasses were used for calibration standards. All elemental concentrations were calculated by applying  $^{29}\text{Si}$  as an internal standard, with Si concentration calculated from the theoretical value of beryl (31.35 wt.%). Laser spots were applied in the same area where UV-Vis spectra were collected, which was usually clean and had an even color dis-

tribution, though color-zoned areas were also sampled (figure 2).

## RESULTS

**Gemological Properties.** The samples' gemological properties are summarized in table 1. The refractive indices varied from 1.570 to 1.588 for  $n_e$  and 1.576 to 1.593 for  $n_w$ , with birefringence between 0.006 and 0.010. Emeralds from Musakashi, Davdar, and all the Colombian deposits had lower RI than the samples from Kafubu and Panjshir. The Musakashi emeralds displayed a particularly strong pink reaction in the Chelsea color filter, while a pink to strong pink display was typical in samples from all other localities except for Kafubu, in which there was no reaction.

**Microscopic Characteristics. Musakashi, Zambia.** In the 11 samples reportedly from Musakashi, the most common inclusions were three-phase, usually con-

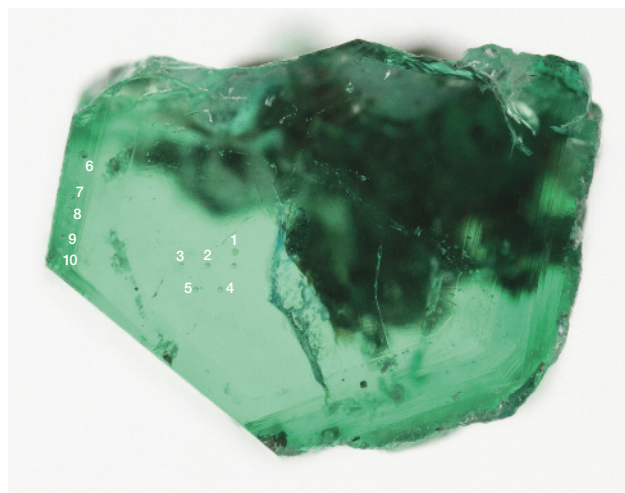


Figure 2. This optical wafer from a Muzo emerald provides an example of the LA-ICP-MS sample points selected in this study. Heavily included areas were avoided in favor of well-crystallized zones in the sample that best represent the chemical composition of that emerald. Photo by S. Engniwat.

taining at least two colorless transparent crystals and a rather small gas bubble suspended in a fluid (figures 3 and 4). Such inclusions were found in every sample we studied. The gas bubble always measured within the size range of the two crystals in the multiphase inclusion. In those inclusions containing two crystals, both crystals appeared to be singly refractive under cross-polarized illumination. The larger crystal was essentially cubic and bright, while the smaller one was rounded and faint (figure 3, A and B). In many samples, the multiphase inclusions also hosted one or more small dark to black crystals, and occasionally tiny colorless or whitish crystals (figures 3 and 4). Some of these inclusions were identified by Raman spectroscopy (figure 4); the gas phase was identified as CO<sub>2</sub> (peaks at 1284 and 1387 cm<sup>-1</sup>). The singly refractive cubic crystals displayed only the emerald spectrum and no Raman lines, suggesting they could be halides (Venkateswaran, 1935). Daughter crystals

were identified as calcite (peaks at 283, 713, and 1085 cm<sup>-1</sup>). An additional peak at 2328 cm<sup>-1</sup> was assigned to N<sub>2</sub>. These results match those for fluid inclusions found in Colombian emeralds (Giuliani et al., 1994), but SEM is needed to identify the different complex mixed salts and daughter minerals. The shape of the inclusions was usually irregular, with numerous branches. In rare cases they appeared needle-like (figure 3C) or jagged (figure 3D).

Under darkfield illumination, tube-like growth features (figure 5) were found in 10 of the 11 Musakashi samples. The tubes were oriented parallel to the prism faces of the crystal, a common feature in emeralds. Each sample had an evenly distributed green color except for one that displayed color banding ranging from strong green to colorless perpendicular to the c-axis and the growth tubes.

Solid inclusions were quite rare. Of the 11 emeralds, only four hosted mineral inclusions that were not part of multiphase inclusions. The most common

## In Brief

- Three-phase inclusions in emerald, once considered a reliable indicator of Colombian origin, have also been observed in specimens from Zambia, Afghanistan, and China.
- Microscopy, spectroscopy, and trace-elemental analysis were used to characterize 84 emeralds with multiphase inclusions.
- A promising basis for determining the geographic origin of emeralds comes from a combination of these methods.

crystal inclusions identified using Raman spectroscopy were colorless and transparent euhedral calcite crystals (figure 6, left). Also found were several opaque and metallic euhedral inclusions resembling

TABLE 1. Gemological properties of emeralds from various sources.

Property	Musakashi, Zambia	Kafubu, Zambia	All Colombia	Davdar, China	Panjshir, Afghanistan
Refractive indices					
n <sub>e</sub>	1.572–1.578	1.582–1.588	1.570–1.573	1.577–1.580	1.572–1.580
n <sub>ω</sub>	1.580–1.582	1.590–1.593	1.576–1.580	1.583–1.588	1.580–1.590
Birefringence	0.006–0.008	0.005–0.008	0.006–0.008	0.005–0.008	0.007–0.010
Chelsea filter	Strong pink	Inert	Pink to strong pink	Pink	Inert to pink

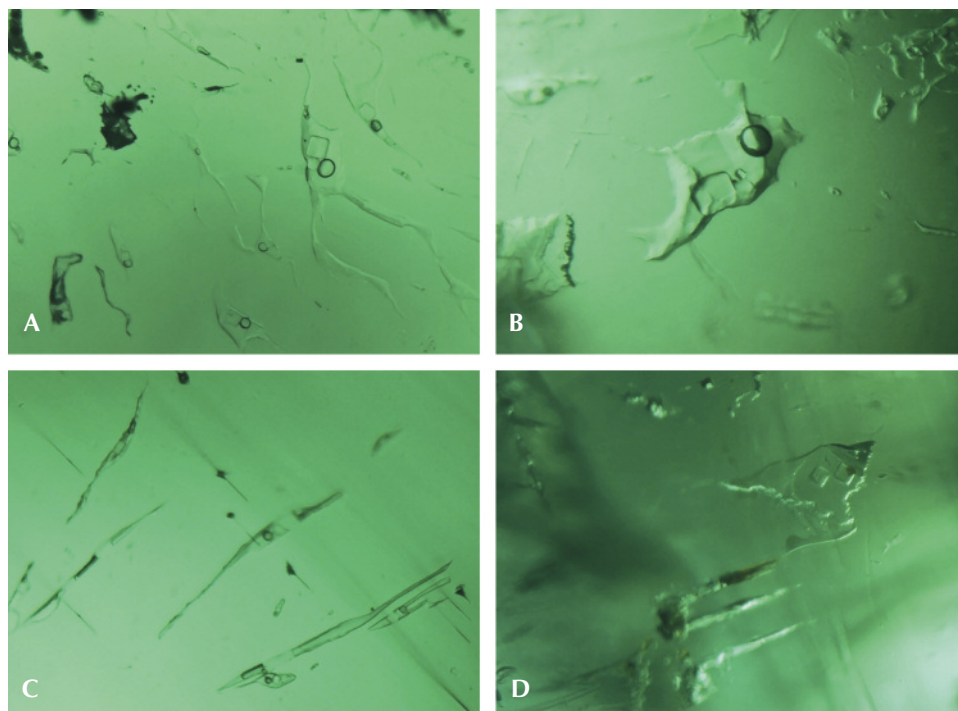


Figure 3. Three-phase inclusions in Musakashi emeralds. A: The larger multi-phase inclusion displays several crystals and a small gas bubble. B: Along with the gas bubble, at least three colorless crystals and one or two tiny dark crystals are visible. C: Two colorless transparent crystals and a small gas bubble in elongated multiphase inclusions. D: Two colorless transparent crystals with a small gas bubble and a tiny black crystal in irregularly shaped multiphase inclusions. Photomicrographs by S. Saeseaw, brightfield illumination. Image widths 9 mm (A) and 7 mm (B–D).

iron oxide, possibly hematite or the martite variety of hematite (figure 6, center), and some whitish translucent crystals identified as cryolite (figure 6, right). The iron oxide minerals identified usually occur in granitic pegmatites, but here they appeared in an emerald that also hosted pyrite and calcite inclusions.

Kafubu, Zambia. Most of the inclusions in the Kafubu samples were multiphase and rectangular in shape (figure 7), but some were quite irregular in outline (figures 8 and 9). These inclusions typically hosted some liquid and a gas bubble, but in several cases it was possible to see a solid third phase. Usu-

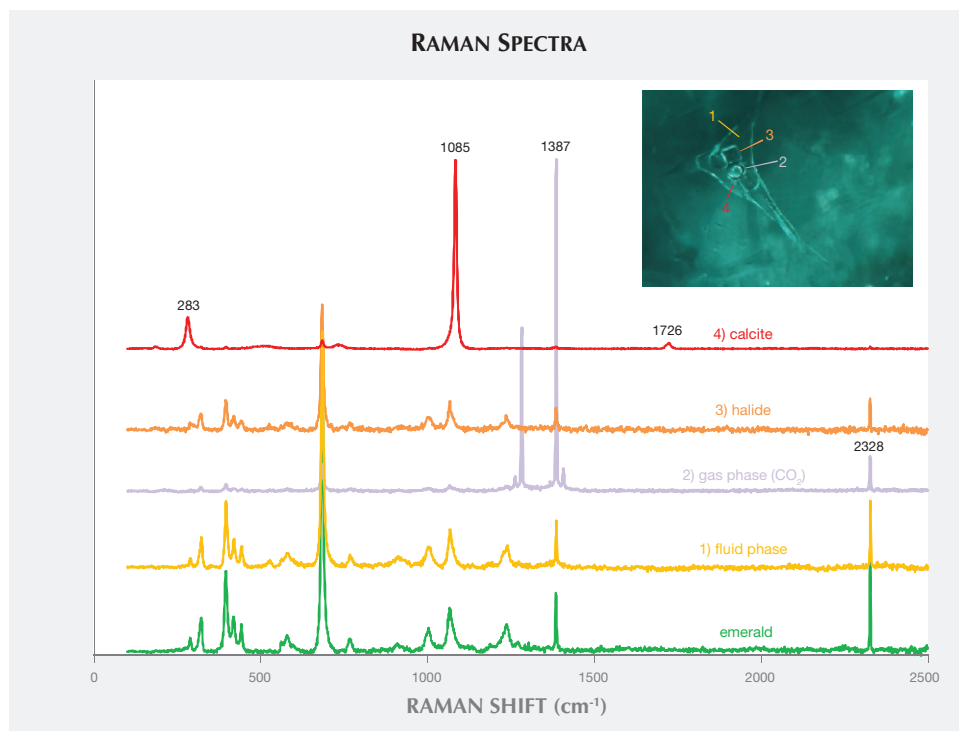


Figure 4. This Musakashi emerald clearly displays a gas bubble, a cubic crystal, two rounded colorless crystals, a tiny black crystal, and two tiny whitish rhombohedra. Raman spectroscopy was used to identify the host emerald (green), the CO<sub>2</sub> gas bubble (purple), the square halide crystal (orange), and the smaller carbonate crystal (red). Photomicrograph by S. Saeseaw; brightfield illumination.



Figure 5. Growth tubes parallel to the prism faces of the crystal are visible in this Musakashi emerald. Photomicrograph by S. Saeseaw, brightfield illumination. Image width 27 mm.

ally the associated crystal had very low relief. When the inclusions were studied between crossed polarizers, the crystal showed evidence of being doubly refractive (figure 9). This was very different from our observations of the Musakashi emeralds, which had at least two singly refractive crystals (halides) trapped within the multiphase inclusions.

Another interesting observation of the Kafubu emeralds was that when the inclusion and the gas bubble were flat, we could estimate the size ratio between them. In these samples, the gas bubble appeared to contain one-third to one-half the volume of the multiphase inclusion at room temperature. This was much larger than the gas bubble observed in emeralds from Musakashi, which indicates considerably different temperature and pressure conditions of formation and possibly very different fluid composition. These observations suggest a different geologic background.

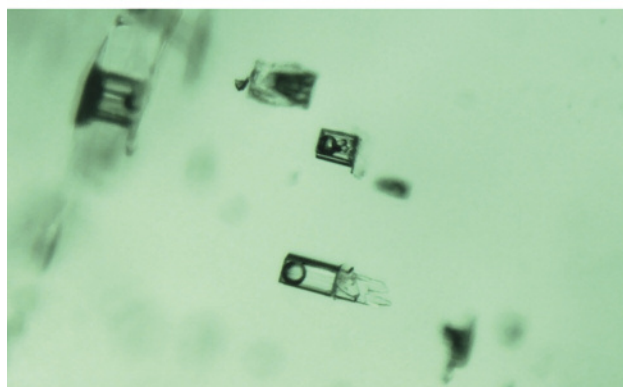
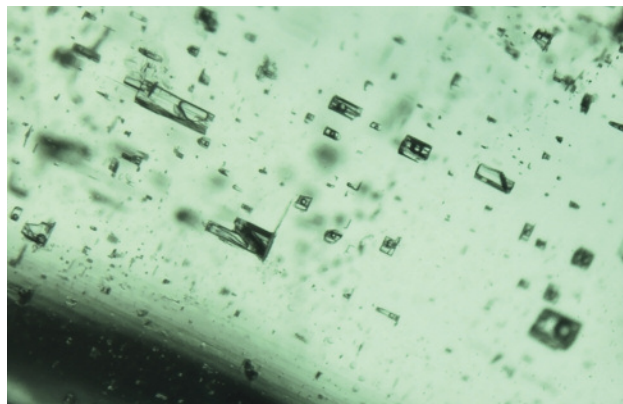
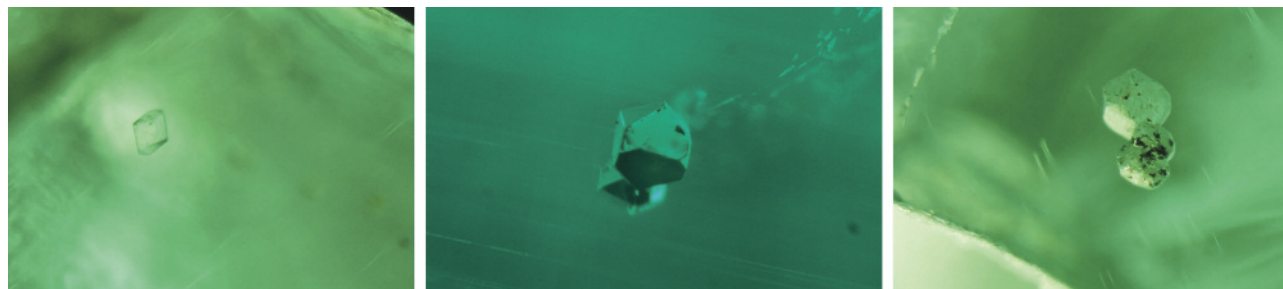


Figure 7. Top: Rectangular multiphase inclusions were visible in emeralds from Kafubu. Bottom: Detail of rectangular multiphase inclusions in an emerald from the Kagem mine reveals relatively large gas bubbles, with and without solid inclusions. Photomicrographs by V. Pardieu, brightfield illumination. Image widths 27 mm (top) and 11 mm (bottom).

Solid inclusions with no associated liquid or gas inclusions were quite common in all the samples from Kafubu. One of the authors (VP) visited Kagem

Figure 6. Single-phase solid inclusions found in the emeralds from Musakashi vary significantly and consist of: a colorless transparent crystal identified by Raman spectroscopy as calcite (left); a metallic opaque crystal, possibly hematite or martite (center); and whitish translucent crystals identified using Raman spectroscopy as cryolite (right). Photomicrographs by S. Saeseaw, darkfield illumination. Image widths 13 mm (left), 11 mm (center), and 10 mm (right).



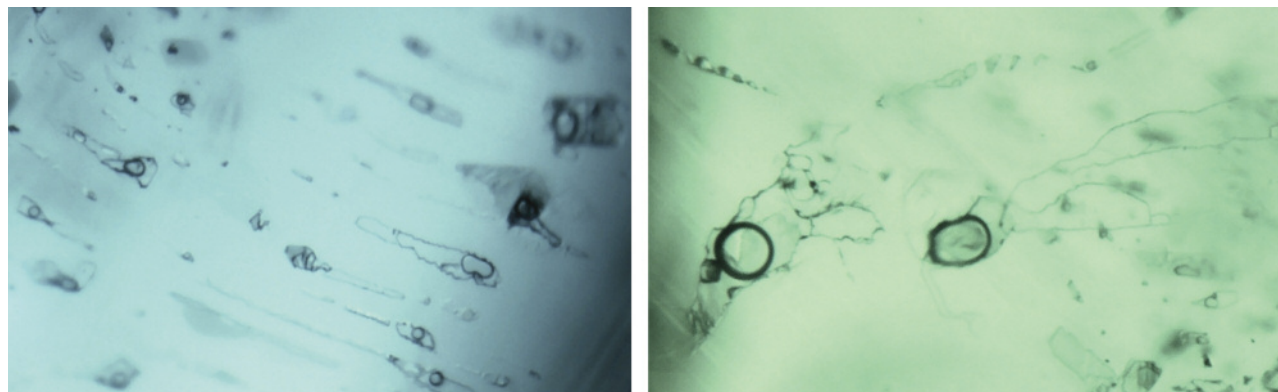


Figure 8. Irregularly shaped multiphase inclusions in emeralds from Kafubu showed liquid containing a gas bubble and in some cases a solid third phase. Photomicrographs by V. Pardieu, brightfield illumination. Image widths 13 mm (left) and 10 mm (right).

in 2011 and 2012 and found that the emeralds there were commonly associated with quartz, pyrite, dark brown to black tourmaline, mica, and chlorite (figure 10). The most common crystal inclusions found had dark, opaque, and dendritic features, identified by Raman spectroscopy as pyrolusite, amphibole, and tourmaline (figure 11), as well as chlorite and mica. These inclusions offer telltale features that reflect the mineral associations found at the site.

*Panjshir Valley, Afghanistan.* Most of the inclusions in emeralds from the Panjshir Valley are multiphase. These typically have an elongated needle-like shape (figures 12 and 13), but they may also display an irregular (figure 14) or even jagged aspect (figure 12). These inclusions often host several cubic to rounded

transparent crystals, and sometimes small, dark opaque crystals. Examined under crossed polarizers, the cubic crystals appeared to be singly refractive and the small rounded crystals appeared doubly refractive (again, see figure 12). These observations were identical to those previously reported (Bowersox et al., 1991). The gas bubble appeared to be smaller than the main crystal inclusion (which was usually cubic).

*Davdar, China.* Most of the inclusions in the samples from Davdar were multiphase. These were often jagged or irregular in shape (figures 15–17) and occasionally needle-like (figure 16). Some fluid inclusions contained two halide cubes (figure 16), as reported previously

Figure 9. Irregular multiphase inclusions in emeralds from Kafubu. Under cross-polarized illumination, a small doubly refractive crystal inclusion becomes visible as a bright spot (see red arrow). Photomicrograph by V. Pardieu; image width 13 mm.

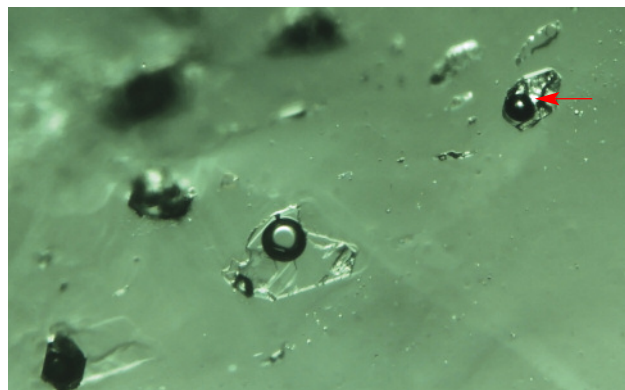
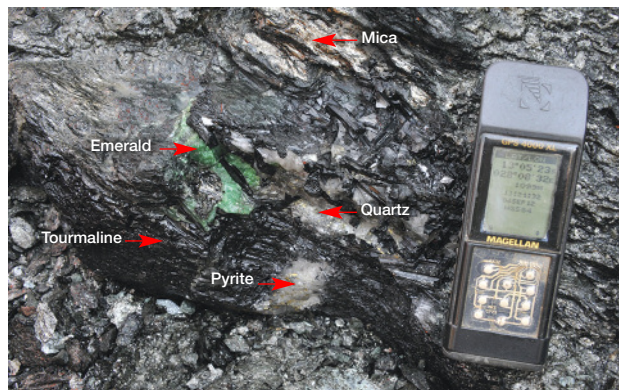


Figure 10. An interesting scene observed at the Kagem mine: an emerald crystal associated with black tourmaline, quartz, mica, and pyrite. It was not surprising to see this mineral association at the site, as it can also be seen inside the gem. This offers a fine example of the direct association between the geological background and the internal world of a gemstone. Photo by V. Pardieu.



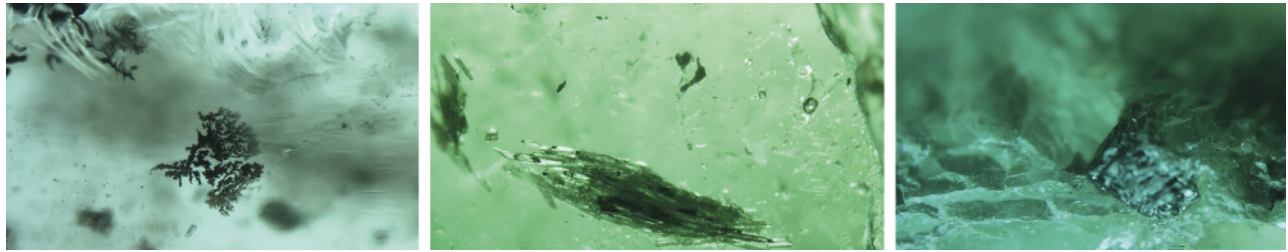


Figure 11. Various single-phase solid inclusions were observed in emeralds from the Kagem mine. Left: A dendritic black opaque mineral inclusion (probably pyrolusite). Center: A dark brownish transparent mineral inclusion identified by Raman spectroscopy as amphibole. Right: A dark brownish mineral inclusion identified as tourmaline with Raman. Photomicrographs by V. Pardieu, brightfield illumination. Image widths 20 mm (left) and 40 mm (center and right).

(Marshall et al., 2012). In these emeralds, the gas bubble was smaller than the whole inclusion and usually somewhat smaller than the associated cubic crystals.

*Colombia.* The most common inclusion in the Colombian emeralds was a jagged multiphase inclusion hosting a gas bubble and one or more cubic crystals (figures 18–20). In these stones, the gas bubble was usually smaller than the whole inclusion and no larger than the associated cubic crystal. Many of these emeralds also contained a tiny dark opaque crystal (figures 18 and 20, right) and clusters of daughter crystals, usually irregularly shaped (figures 19, bottom, and 20, left).

These daughter crystals are related to various carbonate compounds (Giuliani et al., 1994). Most of the multiphase inclusions had the classic jagged shape associated with Colombian emeralds. In several cases the shape was more elongated, like a blade (figure 20, center), and occasionally irregular (figure 20, right).

**UV-Vis-NIR Spectroscopy.** The samples collected for UV-Vis-NIR spectroscopy were fabricated as optical wafers oriented either perpendicular or parallel to the crystal's c-axis—with the exception of emeralds from Musakashi, which were either faceted or contained a single polished window. In this study, UV-Vis-NIR

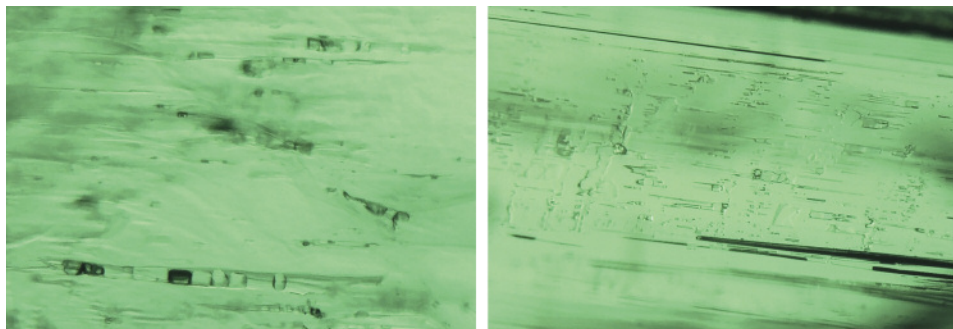


Figure 12. These Panjshir emeralds contain a needle-like multiphase inclusion hosting crystals and gas bubbles (left), and jagged, irregularly shaped multiphase inclusions hosting crystals and gas bubbles (right). Photomicrographs by V. Pardieu, brightfield illumination. Image widths 8 mm (left) and 13 mm (right).

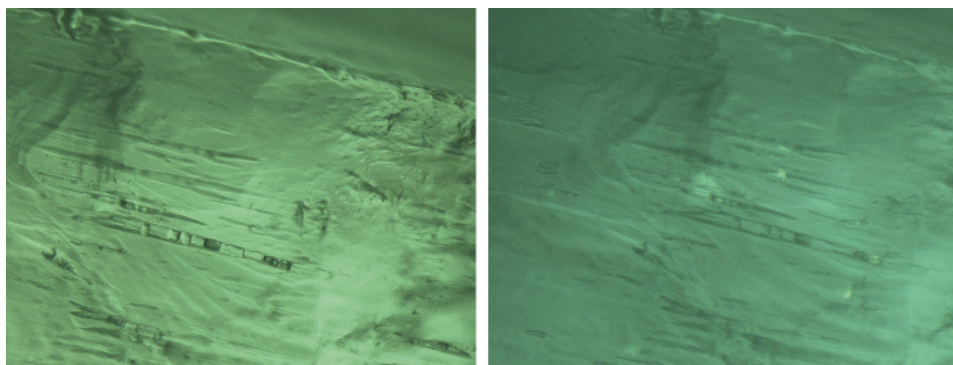


Figure 13. Elongated needle-like multiphase inclusions, hosting several crystals and gas bubbles, in emeralds from the Kamar Safeed area near Khenj in the Panjshir Valley. Photomicrographs by S. Saeseaw, brightfield illumination (left) and crossed polarizers (right). Image widths 9 mm.



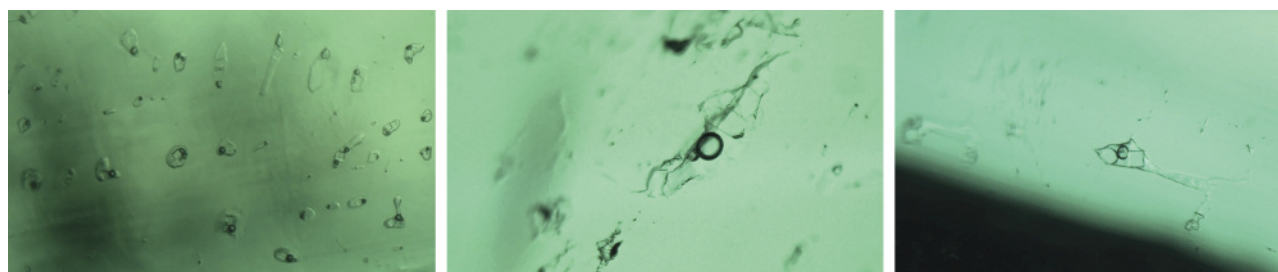


Figure 14. Left: This emerald from the Kamar Safeed area in the Panjshir Valley of Afghanistan contains an irregular blocky multiphase inclusion hosting gas bubbles, a liquid phase, and several crystals. Center: Irregularly shaped multiphase inclusion hosting a gas bubble and several crystals, from the Koskanda area near Khenj. Right: Irregularly shaped multiphase inclusion hosting a small gas bubble and several crystals (one cubic and one more rounded), from Kamar Safeed. Photomicrographs by V. Pardieu, brightfield illumination. Image widths 9 mm (left and center) and 7 mm (right).

spectra characterized the following chromophores for emerald (Wood and Nassau, 1968):

Cation	Identifying absorption characteristic	Possible geographic origin
Cr <sup>3+</sup>	Bands at approximately 430 and 600 nm ( $\omega$ ), and at approximately 420 and 630 nm ( $\epsilon$ ) Lines at 476, 680, and 683 nm	Musakashi, Kafubu, Davdar, Panjshir, Colombia
Fe <sup>2+</sup>	A band at 620 nm ( $\epsilon$ ), and a broad band at approximately 810 nm ( $\omega$ , $\epsilon$ )	Strong: Kafubu Moderate: Davdar, Panjshir
Fe <sup>3+</sup>	Narrow bands at 372 ( $\omega$ ) and 465 nm ( $\omega$ , $\epsilon$ ), and a band at approximately 400 nm ( $\omega$ , $\epsilon$ )	Kafubu, Panjshir
V <sup>3+</sup>	Bands at approximately 400 nm ( $\omega$ ) and 654 nm ( $\epsilon$ )	Strong: Davdar, Colombia

Zambia. In the 11 unoriented samples from Musakashi, the UV-Vis spectra displayed minimum absorptions at about 348 and 510 nm for the ordinary ray. For octahedral Al<sup>3+</sup> in emeralds, substituted Cr<sup>3+</sup> exhibited bands at 430 and 600 nm for the ordinary ray and lines at 476, 680, and 683 nm. These emeralds showed no significant Fe<sup>2+</sup>-related absorption features in the NIR region, and no Fe<sup>3+</sup> was observed (figure 21A).

The nine fabricated samples from Kafubu all displayed the same absorptions: UV-Vis minima at 367 and 514 nm for the ordinary ray, and at 390 and 500 nm for the extraordinary ray. Moreover, a narrow Fe<sup>3+</sup> band was observed at 372 nm in the ordinary ray but not the extraordinary ray, and a strong Fe<sup>2+</sup> band at around at 810 nm was recorded (figure 21B).

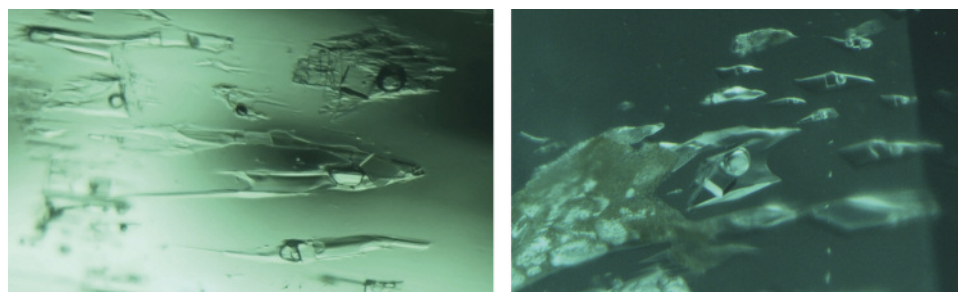


Figure 15. Jagged multiphase inclusions hosting gas bubbles and several crystals in emeralds from Davdar, China. Photomicrographs by S. Saeseaw, brightfield illumination. Image widths 7 mm.

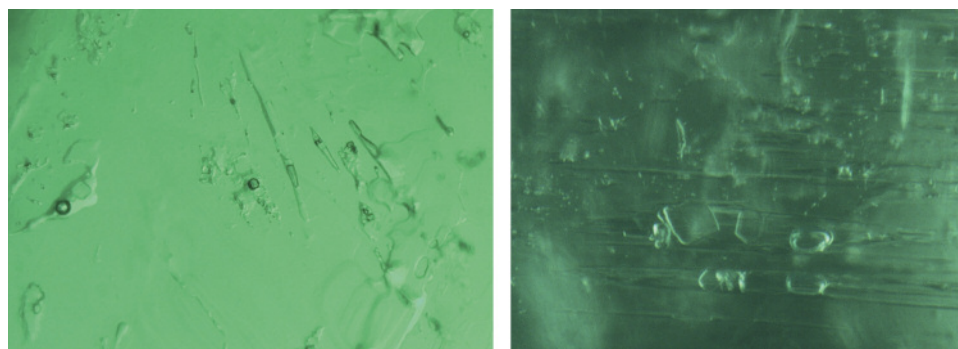


Figure 16. Irregular and needle-shaped multiphase inclusions found in emeralds from Davdar, hosting single gas bubbles, multiple cubic crystals, rounded transparent crystals, and tiny black opaque solids. Photomicrographs by S. Saeseaw, brightfield illumination. Image widths 8 mm (left) and 7 mm (right).

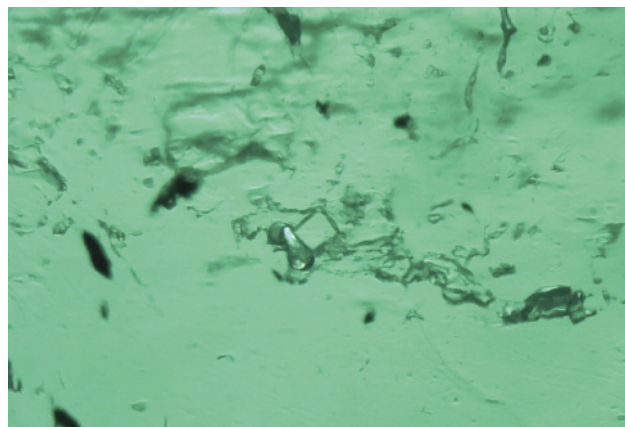


Figure 17. Irregular multiphase inclusions with a gas bubble and a cubic crystal in an emerald from Davdar. Photomicrograph by S. Saeseaw, brightfield illumination. Image width 8 mm.

*Afghanistan.* Nine fabricated samples were studied. Their UV-Vis spectra showed the  $\text{Fe}^{3+}$  peak at 372 nm for the ordinary ray and moderate  $\text{Fe}^{2+}$  absorption at 810 nm, similar to Kafubu emeralds. Yet some of the Panjshir samples appeared to contain no  $\text{Fe}^{3+}$ , due to a low iron concentration, and they also exhibited peak heights at 810 nm that were lower than in the Kafubu samples (figure 21C).

*China.* Ten samples were measured, but only three were fabricated perpendicular or parallel to the c-axis. A representative UV-Vis spectrum is displayed in figure 21D. Davdar and Musakashi emeralds presented similar spectra, but with higher  $\text{Fe}^{2+}$  absorption in the NIR region of the former. But no  $\text{Fe}^{3+}$  features were observed, and strong  $\text{V}^{3+}$  absorptions were detected.

*Colombia.* The eight fabricated samples from Chivor, Coscuez, and Muzo exhibited UV-Vis spectra similar to those of Musakashi emeralds. Neither  $\text{Fe}^{2+}$  nor  $\text{Fe}^{3+}$

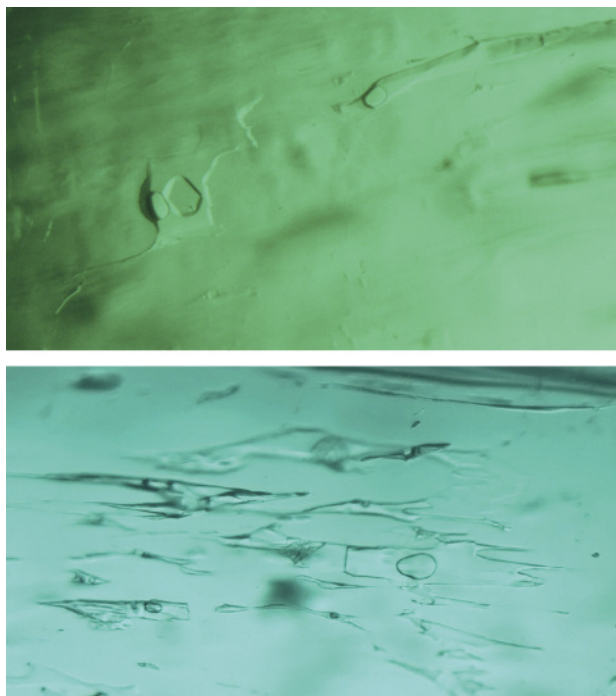


Figure 19. Examples of multiphase inclusions in emeralds from Colombia. Top: This multiphase inclusion hosting a gas bubble and a large colorless cubic crystal with barely visible edges, which appears larger than the bubble, is seen in an emerald from the La Pita area. Bottom: Another example of jagged multiphase inclusions hosting a gas bubble, a large colorless cubic crystal (larger than the bubble), and possibly a smaller cluster of daughter crystals. This sample was from the Coscuez area. Photomicrographs by S. Saeseaw, brightfield illumination. Image widths 9 mm (top) and 10 mm (bottom).

were observed. Absorptions corresponding to  $\text{V}^{3+}$  were present at about 400 and 654 nm (figure 21E).

**FTIR Spectroscopy.** FTIR spectra were recorded in the  $400\text{--}7800\text{ cm}^{-1}$  region, with the major area of

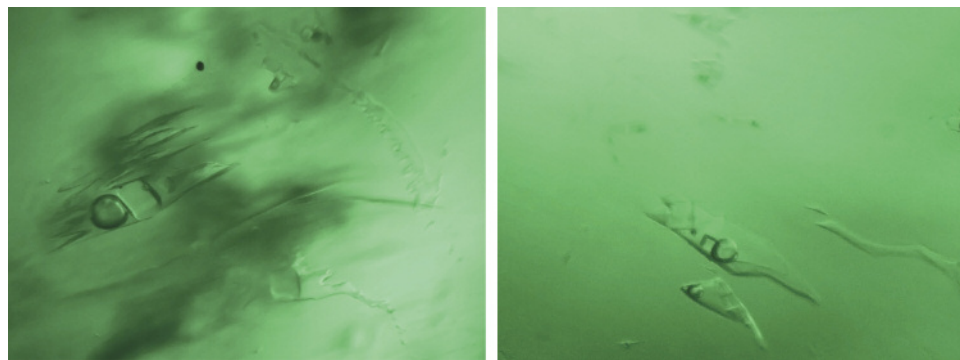


Figure 18. Two classic jagged multiphase inclusions in emeralds from Muzo, Colombia, hosting a gas bubble with two cubic crystals and a tiny dark opaque crystal. Photomicrographs by S. Saeseaw, brightfield illumination. Image widths 9 mm (left) and 7 mm (right).



Figure 20. Left: In Colombian emeralds such as this one from Muzo, liquid was often associated with a gas bubble as well as a large colorless cubic crystal. In this sample, some smaller colorless and dark crystals are also visible. Center: Elongated blade-like multiphase inclusions hosting a gas bubble and a large colorless cubic crystal (slightly larger than the bubble) in an emerald from Coscuez. Right: In some cases, the multiphase inclusions were not jagged or elongated blades but irregularly shaped. Here the multiphase inclusions from a Coscuez emerald host a gas bubble, a large colorless cubic crystal (about the same size as the bubble), and some smaller crystals. Photomicrographs by S. Saeseaw, brightfield illumination. Image widths 13 mm (left) and 8 mm (center and right).

interest between 4500 and 7500  $\text{cm}^{-1}$ —specifically, the area related to water molecule vibrations. The resulting spectra indicated that the emeralds could be divided according to type I and II water molecule assignments (Wood and Nassau, 1968; Schwarz and Henn, 1992). Type I water molecules are oriented in the channels, not linking to other alkali metal ions, and their H-H direction is parallel to the c-axis. Type II molecules are located adjacent to alkali metal ions in the channel, and their H-H direction is perpendicular to the c-axis.

All of the emeralds contained type I water molecules except the samples from Kafubu (figure 22). The extraordinary ray plots of type I emeralds each exhibited a 7140  $\text{cm}^{-1}$  peak that was more intense than the peaks found at 7095 and 7072  $\text{cm}^{-1}$ . The plots from type II emeralds displayed their highest-intensity peak at 7095  $\text{cm}^{-1}$ . These results matched previous reports (Wood and Nassau, 1968; Schwarz and Henn, 1992) that assigned the 7140  $\text{cm}^{-1}$  peak to type I water molecules and the 7095  $\text{cm}^{-1}$  peak to type II water molecules.

**Trace-Element Analysis.** All 84 emeralds from the five different localities were analyzed using LA-ICP-MS (table 2).

**Zambia.** The Musakashi emeralds shared similar trace-element chemistry with the Colombian samples. They contained low concentrations of alkali metals (Li, Na, K, Rb, and Cs); Mg, and Fe, as well as minor traces of Ni. Total alkali ion concentrations averaged 4250 ppmw. In terms of chromophore elements, the concentrations of Cr were greater than V, and the Cr/V ratio ranged between 1.7 and 5.3. Fe

content varied from 680 to 1,490 ppmw. Trace amounts of Ni were also present.

The samples from Kafubu were rich in the trace elements Li, Na, K, Rb, Cs, Mg, and Fe, as well as Ti, Sc, Mn, Ni, and Zn. Total alkali ion concentration was as high as 34,747 ppmw; Mg and Fe contents averaged 15,004 and 8,621 ppmw, respectively. The chromophore elements Cr and V varied from 733 to 4,330 ppmw for Cr and from 71 to 180 ppmw for V; the Cr/V ratio was between 8 and 40. Small amounts of Sc were detected, from 12 to 75 ppmw. Significant traces of Mn, Ni, and Zn were also present.

**Afghanistan.** Afghan emeralds from Panjshir contained on average 10,780 ppmw of alkali ions. The chromophore elements Cr and V ranged from 118 to 4,730 ppmw and from 255 to 3,680 ppmw, respectively. The Cr/V ratio was 0.3 to 3.3. Iron contents ranged from 1,010 to 9,820 ppmw. Scandium contents were detected up to 2,290 ppmw, the highest concentration for this element in our study.

**China.** The emeralds from Davdar contained relatively lower amounts of combined alkali ions, 8,835 ppmw on average. Their green color was caused by the presence of both Cr and V, which varied from 146 to 5,630 ppmw for Cr and from 657 to 6,960 ppmw for V. The ratio for Cr/V was 0.1 to 1.0. Iron concentrations ranged up to 4,350 ppmw.

**Colombia.** All the Colombian emeralds contained low concentrations of alkali metals (Li, Na, K, Rb, and Cs), as well as Mg and Fe. Total alkali ion concentrations averaged 4,725 ppmw. The chromophore elements Cr and V ranged from 172 to 10,700 ppmw for

## UV-VIS-NIR ABSORPTION SPECTRA

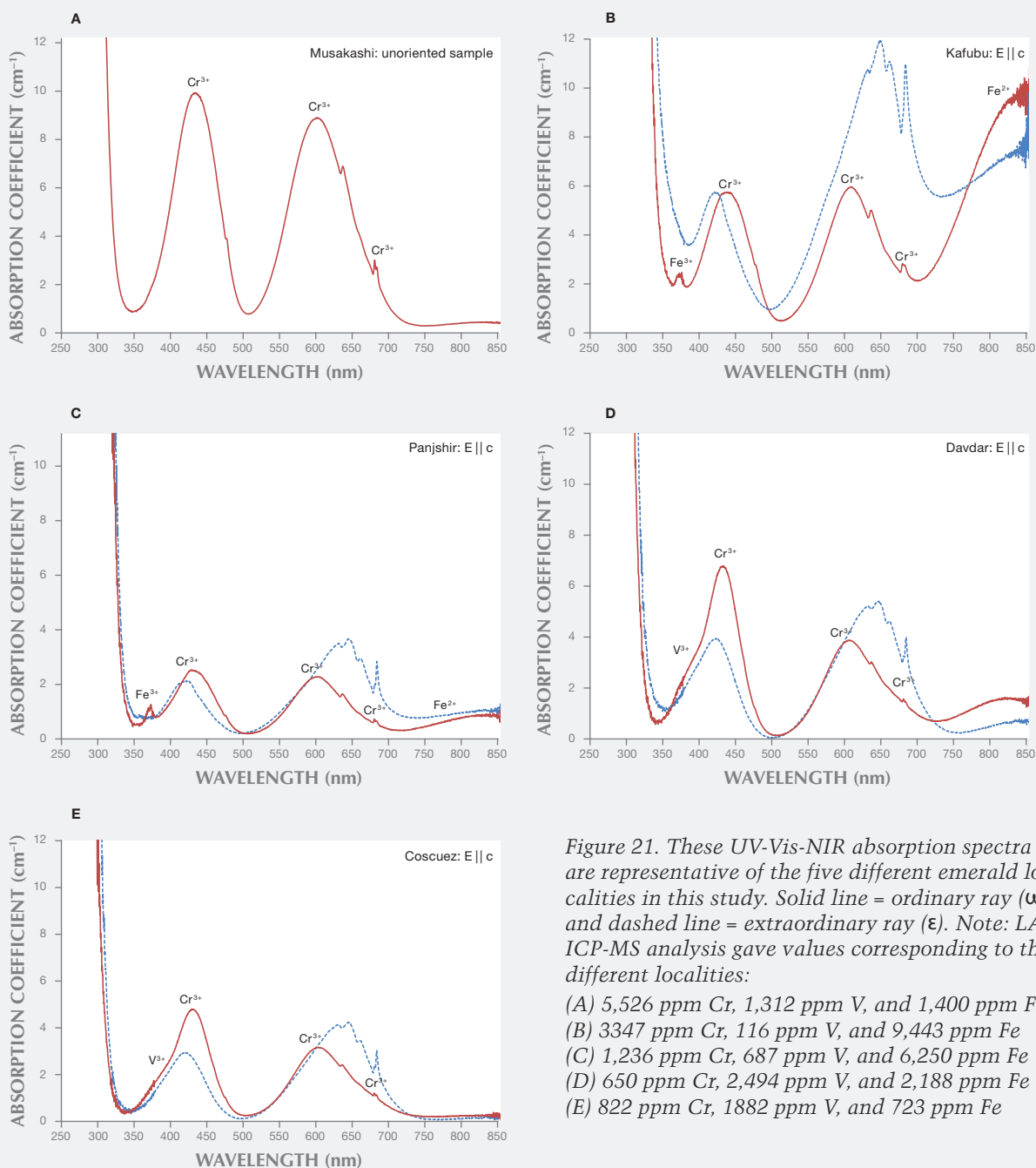


Figure 21. These UV-Vis-NIR absorption spectra are representative of the five different emerald localities in this study. Solid line = ordinary ray ( $\omega$ ) and dashed line = extraordinary ray ( $\epsilon$ ). Note: LA-ICP-MS analysis gave values corresponding to the different localities:

- (A) 5,526 ppm Cr, 1,312 ppm V, and 1,400 ppm Fe
- (B) 3347 ppm Cr, 116 ppm V, and 9,443 ppm Fe
- (C) 1,236 ppm Cr, 687 ppm V, and 6,250 ppm Fe
- (D) 650 ppm Cr, 2,494 ppm V, and 2,188 ppm Fe
- (E) 822 ppm Cr, 1882 ppm V, and 723 ppm Fe

Cr and from 218 to 10,100 ppmw for V; the Cr/V ratio was between 0.04 and 3.5. La Pita contained higher Cr and V than the other Colombian mines. Overall, the Colombian emeralds contained the lowest Fe concentrations in this study, from 117 to 2,030 ppmw.

## DISCUSSION

**Geology.** Several summaries describing the geology of major emerald deposits are available in the gemological and geological literature (Giard, 1998; Behmenburg, 2002; Groat et al., 2008), but very few have dealt

**TABLE 2.** Chemical composition (average ppmw) of 84 emerald samples by LA-ICP-MS.<sup>a</sup>

Element	Musakashi, Zambia	Kafubu, Zambia	Panjshir, Afghanistan	Davdar, China	Coscuez, Colombia	Muzo, Colombia
	11 samples, 55 spots	10 samples, 165 spots	15 samples, 205 spots	13 samples, 103 spots	12 samples, 100 spots	12 samples, 89 spots
<sup>7</sup> Li	55–97 (73)	360–872 (576)	78–254 (113)	72–332 (109)	52–139 (83)	28–92 (45)
<sup>9</sup> Be	40,700–55,6000 (47,260)	40,600–59,000 (49,630)	44,500–57,900 (51,578)	45,800–71,400 (54,515)	45,200–57,100 (50,448)	43,400–56,800 (51,053)
<sup>23</sup> Na	1,150–5,900 (4,109)	14,200–20,100 (17,204)	2,470–15,600 (9,822)	4,200–12,500 (8,356)	2,530–6,500 (4,885)	1,890–9,860 (4,527)
<sup>24</sup> Mg	928–5,740 (3,652)	12,600–17,400 (15,004)	1,790–15,700 (9,197)	3,420–11,700 (7,366)	2,100–5,840 (4,176)	1,720–6,590 (3,869)
<sup>27</sup> Al	75,6000–108,000 (90,895)	64,100–92,400 (77,865)	71,900–110,000 (90,390)	81,200–153,000 (101,220)	83,400–112,000 (94,655)	81,300–109,000 (97,888)
<sup>39</sup> K	25–102 (59)	305–890 (506)	52–1,590 (670)	102–609 (340)	6–46 (14)	7–49 (26)
<sup>45</sup> Sc	40–240 (119)	12–75 (31)	49–2,290 (580)	54–916 (372)	2–258 (41)	34–706 (224)
<sup>51</sup> V	588–2,100 (1,165)	71–180 (109)	255–3,680 (1,444)	657–6,960 (2,867)	656–6,210 (2,204)	673–6,920 (2,062)
<sup>53</sup> Cr	1,340–6,170 (4,211)	733–4,330 (2,287)	118–4,730 (1,832)	146–5,630 (1,333)	172–6,330 (1,156)	208–4,890 (1,620)
<sup>57</sup> Fe	680–1,490 (1,224)	5,900–11,600 (8,621)	1,010–9,820 (3,890)	1,230–4,350 (2,440)	285–1,130 (650)	188–2,030 (588)
<sup>69</sup> Ga	13–29 (20)	9–19 (15)	12–38 (24)	10–43 (23)	13–54 (28)	17–44 (30)
<sup>85</sup> Rb	1–5 (3)	17–105 (65)	4–110 (50)	3–29 (15)	0.7–3 (2)	0.8–5 (3)
<sup>133</sup> Cs	3–10 (6)	527–2,210 (1,391)	11–97 (49)	6–41 (15)	7–19 (12)	4–19 (11)
<sup>47</sup> Ti	bdl–30 (6)	6–25 (12)	bdl–67 (14)	bdl–63 (7)	bdl–27 (6)	bdl–14 (4)
<sup>60</sup> Ni	bdl–12 (6)	7–38 (20)	bdl–14 (2)	bdl	bdl–3 (2)	bdl–3 (1)
<sup>66</sup> Zn	bdl–2 (1)	12–44 (29)	bdl–5 (1)	bdl–8 (2)	bdl–2 (1)	bdl–5 (1)

<sup>a</sup>Data reported in minimum and maximum values, with average concentration in parentheses; ppmw = parts per million by weight; bdl = below detection limit.

with the newer deposits such as Davdar or Musakashi. The mention by Klemm (2010) of sandstone as a possible host rock for Musakashi emeralds is quite interesting, as calcareous sandstone was also identified as the main host rock of the emeralds from Davdar (Pardieu and Soubiraa, 2006; Michelou and Pardieu, 2009; Schwarz and Pardieu, 2009; Marshall et al., 2012). It is

very intriguing to observe similar multiphase inclusions in the stones from these two deposits.

**Multiphase Inclusions.** The discovery of three-phase inclusions in samples reportedly from Musakashi was rather surprising. While these inclusions are similar to those in emeralds from Colombia, Afghan-

Peñas Blancas, Colombia	La Pita, Colombia	Chivor, Colombia	Detection limit
2 samples, 10 spots 30–65 (48)	3 samples, 15 spots 24–80 (44)	6 samples, 35 spots 40–113 (67)	0.2
49,900–54,700 (52,480)	52,900–70,700 (58,666)	46,900–56,000 (50,365)	2.3
2,390–4,100 (3,226)	1,980–7,000 (4,677)	1,340–6,090 (3,448)	8.8
2,280–3,740 (2,888)	1,840–6,830 (4,475)	1,100–5,280 (2,859)	0.4
96,600–109,000 (102,750)	92,300–129,000 (105,493)	84,600–110,000 (97,188)	3.6
8–11 (10)	bdl–40 (24)	bdl–30 (14)	3.0
36–82 (57)	94–344 (248)	6–173 (87)	0.8
317–3,960 (2,000)	6,000–10,100 (8,004)	218–2,020 (846)	0.3
1,810–2,540 (2,183)	2,940–10,700 (5,645)	671–2,880 (1,334)	2.5
164–656 (400)	200–383 (280)	117–862 (366)	18.4
12–30 (20)	32–36 (34)	7–40 (19)	0.1
0.6–1	bdl–4 (3)	0.5–3 (2)	0.1
3–10	5–12	6–16 (11)	0.1
4–7 (4)	bdl–5 (4)	bdl–7 (4)	2.1
bdl	bdl	bdl	0.5
bdl	bdl	bdl	0.4

istan, and China (Xin Jiang), specimens from the neighboring Kafubu area of Zambia contain two-phase inclusions or three-phase inclusions with crystals that are only visible under cross-polarized light (Zwaan et al., 2005). The stones reportedly from Musakashi had multiphase inclusions hosting not only liquid and gas bubbles but also several solid

phases. Usually at least two crystals could be seen: one cubic, one more rounded, and often several smaller ones ranging from transparent colorless to opaque black. This was not typically observed in our Colombian samples. The cubic crystals, the gas phase, and the daughter crystals were identified by Raman spectroscopy as a halide, CO<sub>2</sub>, and carbonate, respectively. These results are identical to those reported for fluid inclusions in Colombian emerald (Giuliani et al., 1994). The shape of the cavity housing the multiphase inclusions in our Musakashi samples was usually quite irregular, not unlike those seen in those from Colombia, Afghanistan, and China. In some cases the cavity's shape was similar to the jagged form commonly found in Colombian emeralds or the elongated needle shape typical of Panjshir emeralds. But for the most part, the cavities in the Musakashi samples were similar to those associated with Davdar.

Unlike the Kafubu emeralds, the multiphase inclusions in our Musakashi samples also contained more crystals with single refraction than double refraction. The gas bubbles in Musakashi multiphase inclusions were smaller than those found in Kafubu material. These results reflect the possibility that different temperature and pressure conditions, geologic backgrounds, and fluid compositions existed when the emeralds from these two neighboring locations formed.

**Spectroscopy.** *UV-Vis-NIR.* The UV-Vis-NIR spectra were characterized by absorptions that resulted from the presence of the chromophores chromium, vanadium, and iron, illustrated in figure 21. The Musakashi emeralds shared similar absorption characteristics with those from Colombia and Davdar, but with lower V<sup>3+</sup> absorption. Furthermore, the Musakashi samples showed no significant Fe<sup>2+</sup>-related absorption features at about 810 nm, and no Fe<sup>3+</sup> absorption at about 372 nm, which distinguished them from Davdar and most of the Kafubu material. Kafubu and Panjshir samples showed a strong narrow absorption band at 372 nm corresponding to Fe<sup>3+</sup>, as well as a broad band around 810 nm corresponding to Fe<sup>2+</sup>. The Davdar emeralds displayed only the Fe<sup>2+</sup>-related broad band. The 810 nm peak is related to Fe content, though their relationship has not been clearly established yet. With higher iron concentration, the peak intensity at 810 nm increased, along with the peak at 372 nm. In this study, we measured the 810 nm peak height of the ordinary ray, which ranged from 7 to 11 cm<sup>-1</sup> (Kafubu) and from 1 to 5 cm<sup>-1</sup> (Panjshir).

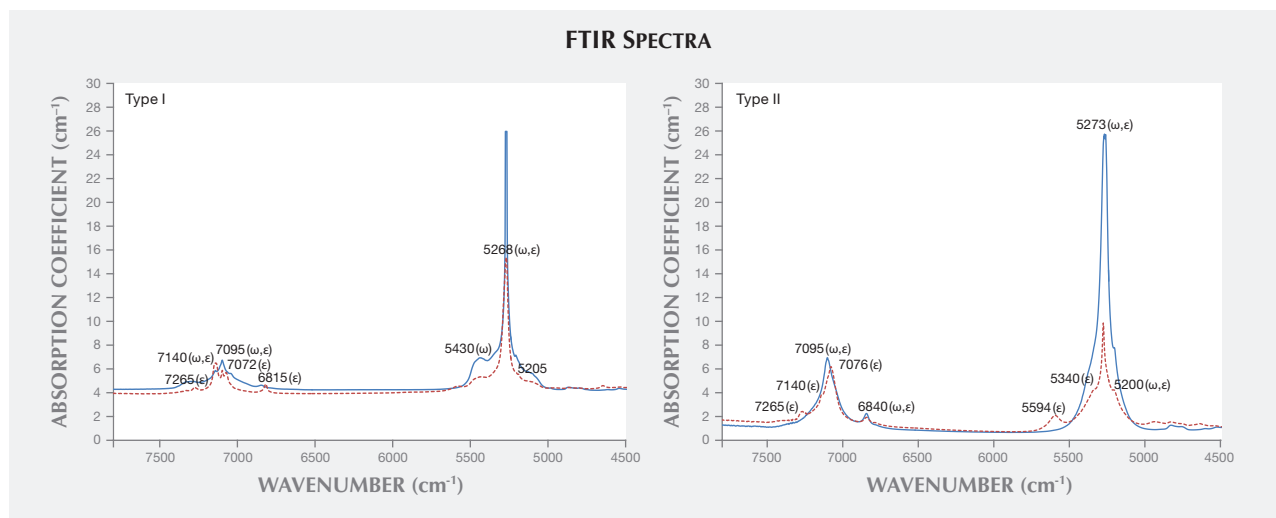


Figure 22. Representative FTIR spectra (solid line = ordinary ray  $\omega$ , dashed line = extraordinary ray  $\epsilon$ ) illustrating the type I and II water observed in emeralds from each origin. Type I samples showed peaks at 7140 ( $\epsilon$ ,  $\omega$ ), 7095 ( $\epsilon$ ,  $\omega$ ), 7072 ( $\epsilon$ ), 7042 ( $\omega$ ), 6843 ( $\omega$ ), 6815 ( $\epsilon$ ), 5430 ( $\omega$ ), 5268 ( $\omega$ ,  $\epsilon$ ), and 5205 ( $\omega$ ,  $\epsilon$ )  $\text{cm}^{-1}$ . Type II samples (which were only from Kafubu) showed peaks at 7265 ( $\epsilon$ ), 7140 ( $\epsilon$ ), 7095 ( $\omega$ ,  $\epsilon$ ), 7076 ( $\epsilon$ ), 6840 ( $\omega$ ,  $\epsilon$ ), 5594 ( $\epsilon$ ), 5340 ( $\epsilon$ ), 5273 ( $\omega$ ,  $\epsilon$ ), and 5200 ( $\omega$ ,  $\epsilon$ )  $\text{cm}^{-1}$ .

**FTIR.** The FTIR spectra recorded for the type I emerald samples all showed a 7140  $\text{cm}^{-1}$  peak, higher than those at 7095 and 7072  $\text{cm}^{-1}$  for the extraordinary ray, related to low alkali metals contents in the channels of the beryl structure. (Again, Kafubu was the only locality that yielded type II samples.) Total alkaline ion concentration, determined using LA-ICP-MS, showed no relationship with the peak at 7140  $\text{cm}^{-1}$ . This was because some of the alkali metals may exist in sites other than those that influence the water spectrum. For example, Li may occur in Be or Si sites, depending on ion sizes.

**Trace-Element Variations.** The samples from Musakashi were characterized by LA-ICP-MS as having low concentrations of alkali metals and Mg, and high Al content. Most of the Kafubu emeralds seemed to have an abundance of the alkali metals Li, Na, K, Rb, and Cs. Various log-log population fields generated from the trace-element data collected (with multiphase inclusions) showed great potential in distinguishing geographic origin (figures 23–25). To explore this further, we added published data for Brazilian emeralds from Rio Grande do Norte (Zwaan et al., 2012), which confirmed the usefulness of this separation criterion. A log-log plot of Li versus Cs content can easily separate the two Zambian deposits (figure 23). The same type of plot can generally distinguish Panjshir and Davdar from Musakashi and Colombian emeralds, even with a small overlapping

area. This plot may also help differentiate between Davdar and Panjshir, as the areas overlap only slightly. We compare this to Schwarz and Pardieu (2009), whose diagram of Ga versus Fe showed nearly complete overlapping between Davdar and Panjshir, rendering it impossible to distinguish between the two locations. As the population fields in the log-log plot of Li vs. Cs overlap for Musakashi and all Colombian emeralds, a plot of Fe vs. K and Fe vs. Ga proved useful in separating between these two origins (figures 24 and 25). In addition, the recorded Ni content was just above the detection limit in emeralds from Musakashi but below the detection limit in most Colombian samples. Average Fe concentrations were highest in samples from Kafubu. Moreover, the Panjshir emeralds contained higher Sc, which was very useful in distinguishing them.

## CONCLUSIONS

For many years, the observation of three-phase inclusions in emeralds was considered a reliable indicator of Colombian origin. But with the arrival in the market of emeralds from Panjshir (Afghanistan), Davdar (China), and Kafubu and Musakashi (Zambia) that may also display three-phase inclusions, origin determination became more complicated. There are some notable differences, however.

Emeralds from the Musakashi deposit are of particular interest, as their internal features are quite different from those found in the well-known deposits

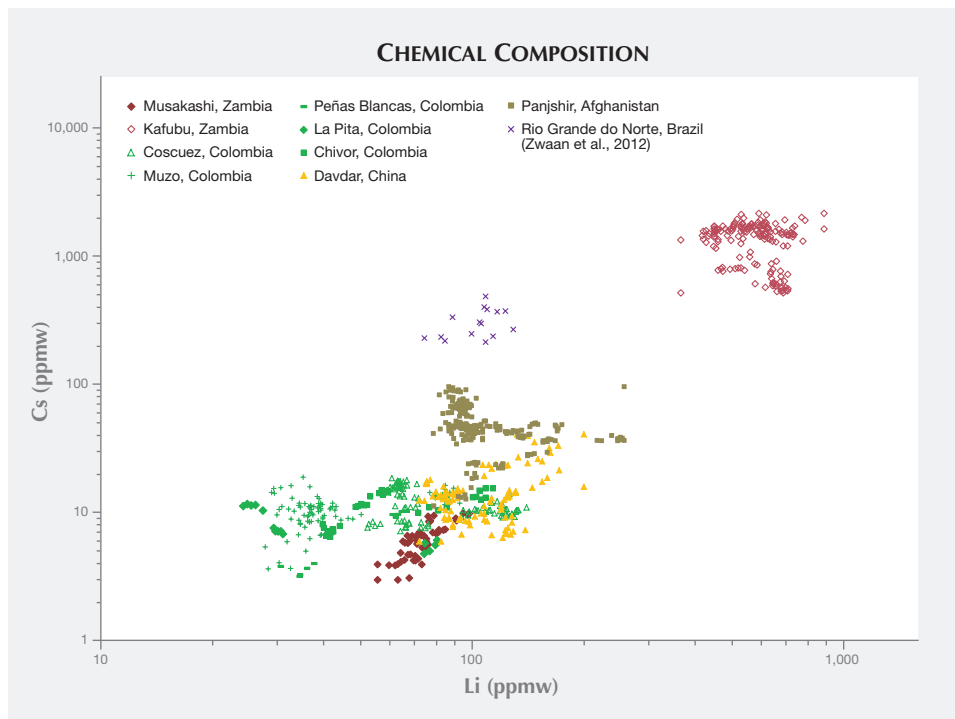


Figure 23. Log-log plot of lithium (Li) versus cesium (Cs) concentrations in emeralds from the five different localities.

in the neighboring Kafubu area. The inclusion scene within the Musakashi emeralds is indeed dominated by multiphase inclusions that are commonly associated with Colombian origin. Nevertheless, the outline and make-up of these multiphase inclusions may be more irregular than those typical of Colombian de-

posits. Furthermore, the tendency of Musakashi emeralds to have at least two crystals associated with a gas bubble may raise questions about a possible Zambian origin.

Emeralds from Panjshir, Afghanistan, are often characterized by elongated needle-shaped multiphase

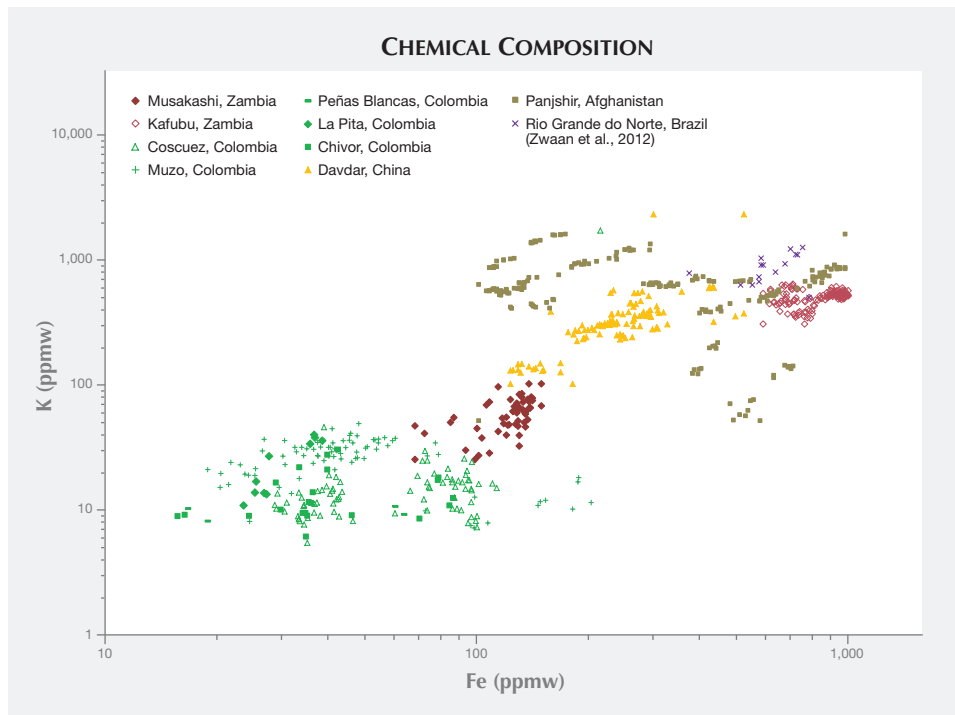


Figure 24. Log-log plot of iron (Fe) versus potassium (K) concentrations in emeralds from the five different localities.



**TABLE 3.** Summary of physical properties, UV-Vis-NIR absorption data, and trace-element chemistry of emeralds from five different localities.

Locality	Refractive index	Color filter reaction	Microscopic characteristics	UV-Vis spectroscopy (cations in addition to Cr <sup>3+</sup> )	Trace-element analysis (84 samples)
Musakashi, Zambia	1.572–1.582	Strong pink	Multiphase inclusions tend to be more irregular than those in Colombian gems; multiphase inclusions with at least two crystals associated with a gas bubble may indicate Zambian rather than Colombian origin	No significant Fe <sup>2+</sup> -related absorption features in the NIR region, and no Fe <sup>3+</sup> observed	Low alkali metal concentrations (1,530–6,060 ppmw) Cr > V; Cr/V ratio 1.7–5.3 Fe concentration: 680–1,490 ppmw Li vs. Cs log-log plot can help separate Musakashi from Kafubu and slightly separate from Colombia Fe vs. K log-log plot can help separate Musakashi from Colombia
Kafubu, Zambia	1.582–1.593 (RI values typically higher than other localities)	Inert	Multiphase inclusions are usually rectangular in shape, but may be irregular in outline; solid crystals of pyrolusite, chlorite, mica, amphibole, and tourmaline	Strong broad Fe <sup>2+</sup> band at approximately 810 nm O-ray: narrow Fe <sup>3+</sup> band at approximately 372 nm	High alkali metal concentrations (15,834–23,294 ppmw) Cr >> V; Cr/V ratio 8–40 Fe concentration: 5,900–11,600 ppmw Li vs. Cs log-log plot can help separate Kafubu from others
Panjshir Valley, Afghanistan	1.572–1.590	Inert to pink	Multiphase inclusions tend to be more elongated or needle-shaped than other localities; each may host several cubic to rounded transparent crystals, and sometimes small, dark opaque crystals	Medium broad Fe <sup>2+</sup> band at approximately 810 nm O-ray: Fe <sup>3+</sup> peak at 372 nm in some samples	Moderate to high alkali metal concentrations (3,946–17,505 ppmw) Cr and V concentrations may be similar: Cr/V ratio 0.3–3.3 Fe concentration: 1,010–9,820 ppmw Li vs. Cs log-log plot can help separate Panjshir from Kafubu, Musakashi, and Colombia (and Davdar, to a lesser extent)
Davdar, China	1.577–1.588	Pink	Multiphase inclusions are usually jagged or irregular in outline, and some are needle-like	Similar to Musakashi: Small broad Fe <sup>2+</sup> band at approximately 810 nm Similar to Colombia: Strong V <sup>3+</sup> bands at approximately 400 and 654 nm	Low to moderate alkali metal concentrations (5,190–12,620 ppmw) Slightly more V than Cr; Cr/V ratio 0.1–1.0 Fe concentration: 1,230–4,350 ppmw Fe vs. K log-log plot can help separate Davdar from Musakashi and Colombia Li vs. Cs log-log plot can help separate Davdar from Panjshir, to a lesser extent
Colombia (Muzo, Coscuez, La Pita, Peñas Blancas, and Chivor)	1.570–1.580 (typically lower than other localities)	Pink to strong pink	Classic jagged multiphase inclusions host a gas bubble and one or more cubic crystals; gas bubbles are usually smaller than the whole inclusion, and also smaller or about the same size as the associated cubic crystal	No Fe <sup>2+</sup> or Fe <sup>3+</sup> observed Weak to medium V <sup>3+</sup> bands at approximately 400 and 654 nm	Low alkali metal concentrations (1,515–8,115 ppmw) Cr and V concentrations may be similar: Cr/V ratio 0.04 and 3.5 Fe concentration: 117–2,030 ppmw Fe vs. Ga and Fe vs. K log-log plot can help separate Colombia from others

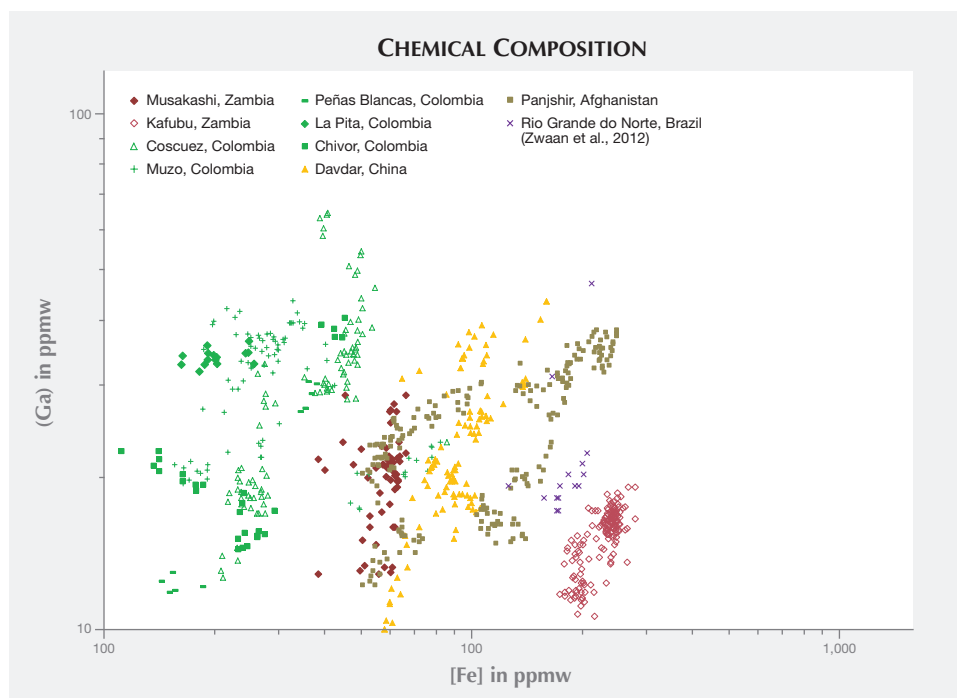


Figure 25. Log-log plot of iron (Fe) versus gallium (Ga) concentrations in emeralds from the five different localities.

inclusions rather than the traditional jagged type often seen in Colombian material. Furthermore, Afghan emeralds often host up to 10 cubic to rounded transparent crystals, and sometimes small dark, opaque crystals. When examined between crossed polarizers, the cubic crystals appeared to be singly refractive and the small rounded crystals appeared doubly refractive. Such features are not typical of Colombian emeralds.

The multiphase inclusions in emeralds from Davdar, China, can be very similar to those in emeralds from Colombian deposits. Many of the multiphase inclusions found in Davdar specimens are jagged and have only one cubic crystal. But the shape of these multiphase inclusions is usually more irregular (sometimes needle-like) than the jagged outline typically observed in Colombian emeralds.

Studying the inclusion scene in these emeralds can be quite confusing, but spectroscopy and trace-element chemistry can provide additional valuable tools to distinguish between them. The presence or absence of  $\text{Fe}^{2+}$  and  $\text{Fe}^{3+}$  and the varying intensity of  $\text{V}^{3+}$  absorption may suggest different countries of origin. More generally, plotting the log-log results from the LA-ICP-MS data for Cs, Li, K, Ga, and Fe resulted in population fields that also appear very promising as a tool in determining the origin of emeralds.

In many cases, the combination of the inclusion scene, UV-Vis-NIR absorption data, and trace-element chemistry (summarized in table 3) can help the gemologist determine the origin of emeralds with three-phase or multiphase inclusions.

#### ABOUT THE AUTHORS

Ms. Saeseaw is a senior manager of colored stones, Mr. Pardieu is a senior manager of field gemology, and Dr. Sangsawong is a research scientist, all at GIA in Bangkok.

#### ACKNOWLEDGMENTS

The authors thank Mr. Guy Clutterbuck for providing Musakashi emeralds. We also thank GIA's Jonathan Moyal for lapidary assis-

tance. John Emmett, Kenneth Scarratt, Emily Dubinsky, and Nathan Renfro provided many helpful discussions. Assistance from Nattida Ng-Pooresatien and Charuwan Khowpong with data collection is also greatly appreciated.

## REFERENCES

- Behmenburg C. (2002) Beryl and emerald: History and myth. In *Extralapis: Emeralds of the World, extraLapis English No. 2*, Lapis International, East Hampton, CT.
- Bowersox G., Snee L.W., Foord E.E., Seal II R.R. (1991) Emeralds of the Panjshir Valley, Afghanistan. *G&G*, Vol. 27, No. 1, pp. 26–39.
- Giard D., Ed. (1998) *L'éméraude*. Association Française de Gemmologie, Paris.
- Giuliani G., Cheillett A., Dubessy J., Rodriguez C.T. (1993) Chemical composition of fluid inclusions in Colombian emerald deposits. *8th Quadrennial IAGOD Symposium*, pp. 159–168.
- Groat L.A., Giuliani G., Marshall D.D., Turner D. (2008) Emerald deposits and occurrences: A review. *Ore Geology Reviews*, Vol. 34, No. 1-2, pp. 87–112, <http://dx.doi.org/10.1016/j.oregeorev.2007.09.003>.
- Hammarstrom J.M. (1989) Mineral chemistry of emeralds and some associated minerals from Pakistan and Afghanistan: An electron microprobe study. In A.H. Kazmi and L.W. Snee, Eds., *Emeralds of Pakistan: Geology, Gemology & Genesis*. pp. 125–150.
- Klemm L. (2009) Fieldtrip to emerald mines in Zambia, summer 2009. From [http://www.gubelingemlab.ch/PDF/Fieldtrips/2009\\_Field\\_report\\_LK\\_Zambia\\_forInternetx.pdf](http://www.gubelingemlab.ch/PDF/Fieldtrips/2009_Field_report_LK_Zambia_forInternetx.pdf).
- (2010) Fieldtrip to emerald mines in Zambia, summer 2010. From [http://www.gubelingemlab.ch/PDF/Fieldtrips/2010\\_Field\\_report\\_LK\\_Zambia\\_Internet.docx.pdf](http://www.gubelingemlab.ch/PDF/Fieldtrips/2010_Field_report_LK_Zambia_Internet.docx.pdf).
- Marshall D., Pardieu V., Loughrey L., Jones P., Xue G. (2012) Conditions for emerald formation at Davdar, China: Fluid inclusion, trace element and stable isotope studies. *Mineralogical Magazine*, Vol. 76, No. 1, pp. 213–226, <http://dx.doi.org/10.1180/minmag.2012.076.1.213>.
- Michelou J.-C., Pardieu V. (2009) A glimpse of the new fine emerald deposit at Xinjiang's Davdar Mine. *InColor*, No. 10, Spring, pp. 26–28, 30.
- Pardieu V., Soubiraa G. (2006) From Kashmir to Pamir, Summer 2006: Gemmological expedition report to ruby, emerald and spinel mining areas in Central Asia. Part 4: China (Xin Jiang): Emeralds from the silk roads. <http://www.fieldgemology.org/gemology%20china%20emerald%20davdar.php>.
- Schwarz D., Henn U. (1992) Emeralds from Madagascar. *Journal of Gemmology*, Vol. 23, No. 3, pp. 140–149.
- Schwarz D., Pardieu V. (2009) Emeralds from the Silk Road countries – A comparison with emeralds from Colombia. *InColor*, No. 12, Fall/Winter, pp. 38–43.
- Schwarz D., Mendes J.C., Klemm L., Lopes P.H.S. (2011) Emeralds from South America – Brazil and Colombia. *InColor*, No. 16, Spring, pp. 36–46.
- Venkateswaran C.S. (1935) The Raman spectra of some metallic halides. *Proceedings of the Indian Academy of Sciences – Section A*, Vol. 1, No. 11, pp. 850–858.
- Wood D.L., Nassau K. (1968) The characterization of beryl and emerald by visible and infrared absorption spectroscopy. *American Mineralogist*, Vol. 53, May-June, pp. 777–799.
- Zwaan J.C., Seifert A.V., Vrána S., Laurs B.M., Anckar B., Simmons W.B., Falster A.U., Lustenhouwer W.J., Muhlmeister S., Koivula J.I., Garcia-Guillerminet H. (2005) Emeralds from the Kafubu area, Zambia. *G&G*, Vol. 41, No. 2, pp. 116–148.
- Zwaan J.C., Jacob D.E., Häger T., Cavalcanti Neto M.T.O., Kanis J. (2012) Emeralds from the Fazenda Bonfim region, Rio Grande do Norte, Brazil. *G&G*, Vol. 48, No. 1, pp. 2–17, <http://dx.doi.org/10.5741/GEMS.48.1.2>

For online access to all issues of GEMS & GEMOLOGY from 1934 to the present, visit:

[gia.edu/gems-gemology](http://gia.edu/gems-gemology)